DOI: 10.3969/j.issn.1673-5188.2017.03.006
http://kns.cnki.net/kcms/detail/34.1294.TN.20170912.1644.004.html, published online September 12, 2017

High Performance Optical Modulator and Detector for 100 Gb/s Transmission System

ZHONG Fang [1], GONG Pan [1], ZHOU Zhiping [1], HUA Feng [2], and WANG Huitao [2]

(1. State Key Laboratory of Advanced Optical Communication Systems and Networks, School of Electronics Engineering and Computer Science, Peking University, Beijing 100871, China;
2. Wireline Product Operation, ZTE Corporation, Beijing 100191, China)

Abstract

Silicon photonics, one of the most promising candidates for breaking the bottleneck of current optical transmission systems, has been developing rapidly in both performance and maturity. The analysis and design of the two key components of this technology, the optical modulator and detector, are presented in this paper. The Mach-Zehnder modulator with U-type PN junction is optimized to obtain the modulation efficiency of 0.559 V·cm. The electro-optical 3 dB bandwidth of this device is 30 GHz. The simulation of the PIN waveguide Si based Ge photodetector at 1.55 μm wavelength is also presented. The device shows a very low dark current of about 10 nA at -1 V, and the obtained responsivity and 3 dB bandwidth are appreciable. These results practically meet the requirement of commercial 100 Gb/s optical transmission systems.

Keywords

silicon photonics; modulator; detector

1 Modulation and Detection in Silicon

Traditional copper interconnects have fundamental limitations such as high loss, crosstalk, and low speed [1]–[3]. Such limitations stem from the properties of electrons and therefore make it increasingly difficult and costly to improve copper interconnects. On the other hand, using photons as the carrier of information evades the problems of electrons with excellent potential for several orders of magnitude higher capacity utilizing wavelength division multiplexing (WDM). As a result, the combined integration of electronic and photonic circuits is poised to break through the interconnection bottlenecks in data networks and on-chip interconnections [4]–[6]. Silicon photonics is currently the leading candidate technology to meet the growing demand for network interconnection capacity and speed. Its compatibility with complementary-metal-oxide-semiconductor (CMOS) fabrication process has positioned this technology towards large-scale and dense integration, high reproducibility and low fabrication costs.

Global information communications require optical transmission systems with high spectral efficiency, high channel data rate, and low cost [7]–[9]. Coherent optical transmission has become a solution for high-capacity long-haul communications with channel data rates at 100 Gb/s and beyond [9]–[11], which employs polarization-division-multiplexed quadrature phase-shift keying (PDM-QPSK). Next-generation transport networks may utilize even higher-level modulation formats, such as 16-ary quadrature amplitude modulation (16-QAM). The soaring complexity poses a challenge to current fiber communication systems but at the same time creates opportunities for the versatile silicon photonics.

As one of the most important components in optical interconnection or communication system, silicon optical modulators have undergone significant development in recent years. Many modulation mechanisms were put forward, and the modulation speed increased from megahertz to multi-gigahertz regime [12]–[21]. The power consumption decreased to femto Joules. A modulator is the device for modulating optical parameters such as amplitude, phase and polarization and transforming the electrical signal to the optical signal. Compared with directly modulating optical sources, external modulation using the modulator has several advantages [16]. The optical sources can be cheaper without internal modulation and the modulation speed can be higher. Phase modulation and higher formats are possible, and it can reduce the power budget in multiple channels system with a single light source feeding. In this work, we focus on electro-optic modulators. The real and imaginary part of material refractive index (RI) may be changed when electric field is applied [17]. Depending on which part of refractive index changed, modulators are categorized into electro-refractive (Δn) and electro-absorptive ($\Delta\alpha$). Major electro-optic effects involving Pockels effect, Kerr effect, and Franz–Keldysh effect are used in traditional modulators to change the material RI. Generally, RI is related to the applied electric field in the following relation:

$$n' = n + a_1|E| + a_2|E|^2 + a_3|E|^3 + \cdots, \tag{1}$$

where n' is the RI of the materials when the electric field is applied, n is the RI without applied electric field, and a_1, a_2, a_3 are the different coefficients of different electro-optic effects. The Pockels effect and Kerr effect are described as $\triangle n = a_1 E$

This work is partially supported by ZTE Industry-Academia-Research Cooperation Funds.

D:\EMAG\2017-08-58/VOL15\RP3.VFT——6PPS/P1

and $\Delta n=a_2E^2$, respectively. As one of the most successful commercial modulators, Lithium niobate modulator operates via Pockels effect and exhibits favorable characteristics, especially high speed. However, the electro-optic effects mentioned above are inconsequential in pure silicon at the telecommunications wavelengths of 1.3 μm and 1.55 μm [5]. Besides, silicon has strong thermo-optic effects, but it is too slow to meet the speed requirement for modern telecommunications applications [18]. To date, most modulators based on silicon use the plasma dispersion effect to achieve modulation. The plasma dispersion effect describes the changes of both RI and absorption of silicon in response to the concentration variation of free carriers as follows [19]:

$$\Delta n=-\frac{q^2\lambda^2}{8\pi^2c^2\varepsilon_0 n_0}\left(\frac{\Delta N_e}{m_{ce}^*}+\frac{\Delta N_h}{m_{\mathrm{ch}}^*}\right),$$
$$\Delta\alpha=\frac{q^3\lambda^2}{4\pi^2c^3\varepsilon_0 n_0}\left(\frac{\Delta N_e}{m_{ce}^{*2}\mu_e}+\frac{\Delta N_h}{m_{\mathrm{ch}}^{*2}\mu_h}\right), \tag{2}$$

where Δn is the refractive index change, $\Delta\alpha$ is the absorptive index change, q is the charge on an electron, λ is the wavelength of the incident light, c refers to the speed of light in vacuum, ε_0 refers to the electric constant in vacuum, n_0 refers to the refractive index of intrinsic silicon, $\Delta N\varepsilon$ refers to the concentration variation of electron, ΔN_h refers to the concentration variation of hole, μ_ε refers to electron mobility, and μ_h refers to hole mobility. Besides, $m_{ce}^*=0.26m_0$, which refers to the effective mass of hole, while $m_{\mathrm{ch}}^*=0.39m_0$, which refers to the effective mass of electron.

To convert phase modulation of plasma dispersion effect to intensity change, either Mach–Zehnder interferometers (MZI) or resonant structures can be adopted. Limited by its narrow band characteristic, resonant modulators suffer from high susceptibility to fabrication errors and temperature variation. For example, 1 nm increase in the average width of the ring waveguide induces 0.25 nm resonant wavelength shift. Owing to the large thermo-optic coefficient of silicon, resonant modulators are extremely temperature-sensitive. On the other hand, Mach–Zehnder modulators are free from these problems. The performance of Mach–Zehnder modulators are hardly affected by changes in temperature and fabrication process, compared with resonant modulators.

Silicon photodetectors are also one of the essential components in the optical transmission and interconnection system. They convert the incident modulated light into electrical signals, and can be used to either monitor light intensity variations or detect high speed optical signals. In recent years, many high performance photodetectors have been demonstrated [20]–[22].

For long-distance optical transmission applications, the 1.55 μm wavelength range is usually used due to the minimum loss window of silica optical fiber. Consequently, photodetectors working in the 1.55 μm wavelength range have been pursued by researchers ever since. Due to a large bandgap of 1.12 eV, bulk Si material demonstrates a limited maximum absorption wavelength of 1.1 μm. However, in order to make full use of the mature CMOS technology, people also tried to fabricate the hetero-junction photodiodes (PDs) by bonding or epitaxying III-V material on the Si substrate, but their advantages seem not prominent [23].

Ge can demonstrate much higher optical absorption in 1.55 μm wavelength range than silicon, due to the smaller bandgap of 0.67 eV. In addition, Ge, as a group IV material, is the same with silicon; its fabrication process can be compatible with the CMOS technology. Thanks to these advantages, Ge photodetectors are becoming the most promising candidates for Si photonics integration.

Both evanescent [20]–[22] and butt [23] coupling schemes have been used to couple light from silicon waveguides to Ge layers. When integrated with small core waveguides, Ge photodetectors have the advantages of easier power transferring to Ge films and fabrication process in the evanescent coupling case.

The commercial 100 Gb/s optical transmission systems traditionally employ the discrete devices, which leads to low stability and high cost. In this work we present the analysis and design of the silicon Mach-Zehnder modulator and Ge PIN waveguide photodetector, whose performance could meet the requirement of the commercial usage and their design and appearance are aligned with large scale integration. Since PDM-QPSK modulation formats are frequently employed in the 100 Gb/s coherent system, which composed by several modulators and detectors, the goal of this work is to design the devices having high performance at more than 25 Gb/s.

2 Performance Metrics

Several metrics can be used to evaluate the performance of modulators and photodetectors. The most important ones are modulation bandwidth, modulation efficiency $V_\pi L_\pi$, and extinction ratio for modulators. Dark current, responsivity, and 3 dB bandwidth are usually used to describe the performance of photodetectors.

Modulation bandwidth is characterized as the frequency at which the modulation is reduced to 3 dB point. This metric is vital to measure the available information capacity of optical modulator.

$V_\pi L_\pi$ is usually used to evaluate the modulation efficiency of MZI modulators. V_π is the half-wave voltage, and L_π is the length of the modulation arm when the device realize π phase. The smaller $V_\pi L_\pi$ means higher modulation efficiency and more compact footprint.

Extinction ratio is the metric to evaluate the modulation depth. It is defined as the ratio of I_{max}, the maximum transmitted intensity when the modulator works in on-state, to I_{min}, the minimum transmitted intensity when the modulator works in off

-state.

For photodetectors, dark current is the reverse bias current when there is no light incidence on the device. It can reflect the leakage current of the device. The smaller the dark current is, the better performance the device has.

Responsivity is the parameter that tells how the photodetector responses to the incident light and converts it into electrical signals. It (R) can be defined as the ratio of the generated current (I) and the incident power (P) of the light, which can be written as $R=I/P$.

The 3 dB bandwidth is used to describe the device performance in the high speed detection systems, and it is characterized to be the frequency at which the detection responsivity is reduced to the 3 dB point.

In the following two sections, we present the simulation process of the silicon Mach-zehnder modulator and PIN waveguide photodetector which can work well in the commercial 100 Gb/s optical transmission system. For the practical application, all the devices should have 23 GHz bandwidth. The extinction ratioof the modulator is required to be larger than 20 dB, the insertion loss should be less than 5 dB when the driving voltage is 3.3 V_{pp}. The responsivity of photodectector should be larger than 0.65 A/W and the dark current is less than 20 nA under 3.3 V_{pp} driving.

3 Design of Silicon Mach-Zehnder Modulator

For single mode propagation, the height and the width of the rib waveguide are chosen to be 220 nm and 500 nm. Through simulating the above single-mode waveguide with different distances between the high doping and the edge of the rib waveguide (defined as L shown in **Fig. 1**) by COMSOL Multiphysics, the limiting factors of the optical energy in the rib waveguide (Q1) and the limiting factors of the optical energy in the rib waveguide and the L region (Q2) are acquired. We find that the Q1 and Q2 are nearly unchanged when L changes from 400 nm to 1000 nm. For decreasing the absorption loss caused by the high doping area, we choose the L of 1000 nm. Based on the above structure, we then optimize the thickness of the slab, H_{slab} in the same way. At last we chose the H_{slab} of 70 nm.

The modulation efficiency can be improved by increasing the overlapping area between the optical field and the depletion area. The U-type PN junction is a good candidate as shown in Fig. 1. The p-type doping concentration is 1×10^{18}/cm^3, and it is the same for the N-type doping. The parameters W_2 and H_2 have more influence on the modulation efficiency. The change of the modulation efficiency with W_2 and H_2 are illustrated in **Fig. 2**. According to the simulated results, when W_2=300 nm, H_2=80 nm, the PN junction can realize the highest efficiency of $V_\pi L_\pi$=0.559 V·cm. The structure's absorption coefficient α is 14.74 dB/cm. When the driving voltage is 3.3 V, the change of absorption loss is 7.64 dB/cm.

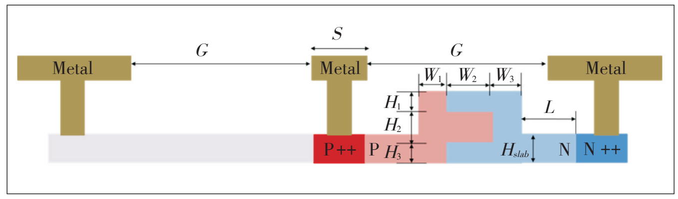

▲**Figure 1. The cross-section diagram of U-type PN junction.**

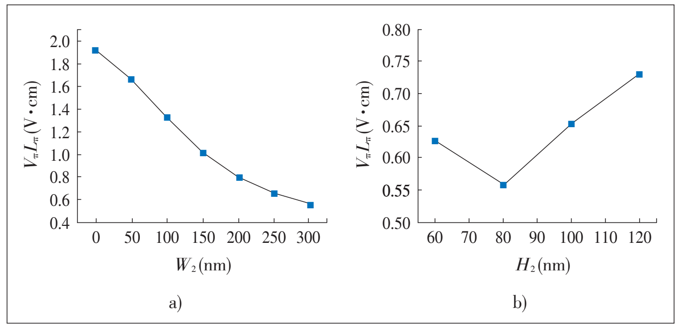

▲**Figure 2. The curves of modulation efficiency of a) W_2 and b) H_2.**

In an asymmetric device, the modulator is on OFF state with 0 V driving voltage which can be tuned by the working wavelength or the statistic phase shifter, and then is on ON state when the device's driving voltage is on. Considering the limited driving voltage of the practical systems, we assume the driving voltage is 3.3 V_{pp}. Since the absorption coefficients of two arms are different, the insertion loss of the MZI structure can be expressed as follows:

$$IL=10\log\left(\frac{I_{out-on}^2}{I_{in}^2}\right), \tag{3}$$

$$I_{out-on}=T_{0V}I_1+T_{3.3V}I_2+2\sqrt{T_{0V}T_{3.3V}}\sqrt{I_1I_2}\cos(\Delta\phi) . \tag{4}$$

Meanwhile, the extinction ratio can be defined as follows:

$$ER=10\log\left(\frac{I_{out-on}}{I_{out-off}}\right), \tag{5}$$

$$I_{out-off}=T_{0V}(I_1+I_2-2\sqrt{I_1I_2}), \tag{6}$$

where I_{in} is the input optical intensity; I_{out-on} and $I_{out-off}$ are the output optical power on ON and OFF state; I_1 and I_2 are the optical intensity of the two arms. Besides, T_{0V}, $T_{3.3V}$ are the absorption coefficients on the driving voltage of 0 V and 3.3 V. When the length of the device is larger than 700 μm, the insertion loss of ON state is less than 4.7 dB. The extinction ratio is also influenced by the beam splitting ratio of the two arms, when the beam splitting ratio is better than 45:55 (I_1 : I_2), the extinction ratio is larger than 20 dB as shown in **Fig. 3**.

Next, we set up the travelling-wave electrode mode using the commercial simulation software High Frequency Structure Simulator (HFSS). The main parameters of the travelling-wave

D:\EMAG\2017-08-58/VOL15\RP3.VFT——6PPS/P3

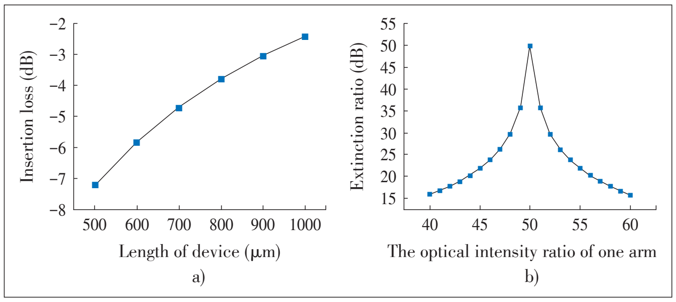

▲**Figure 3. a) The insertion loss vs. the length of the modulation arm; b) the extinction ratio vs. the optical intensity ratio of one modulation arm.**

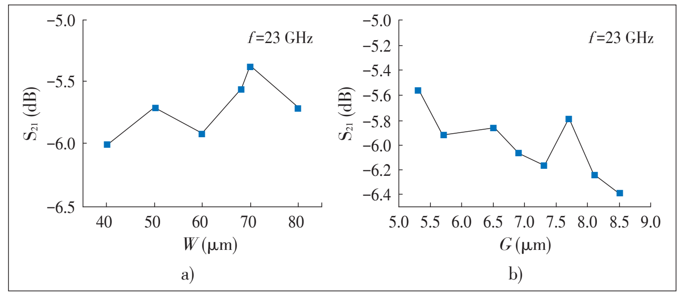

▲**Figure 4. The curves of S_{21} vs. a) *W* and b) *G*.**

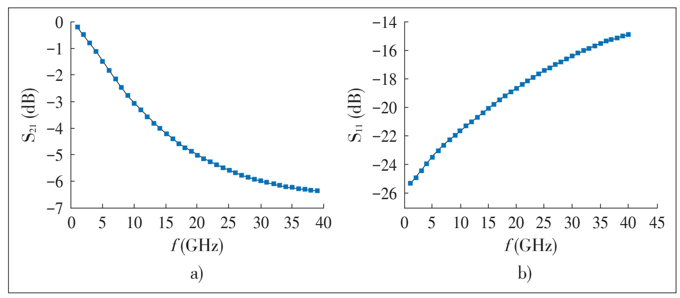

▲**Figure 5. The curves of a) S_{21} and b) S_{11} of the designed electrode.**

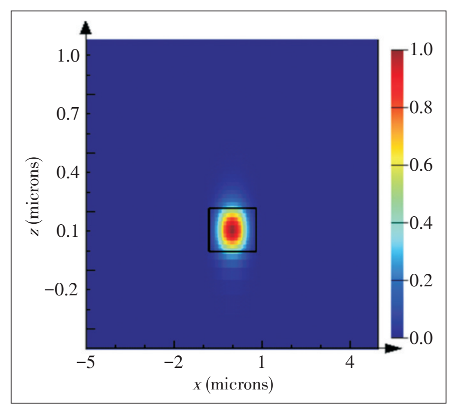

Figure 6.▶ **TE fundamental mode.**

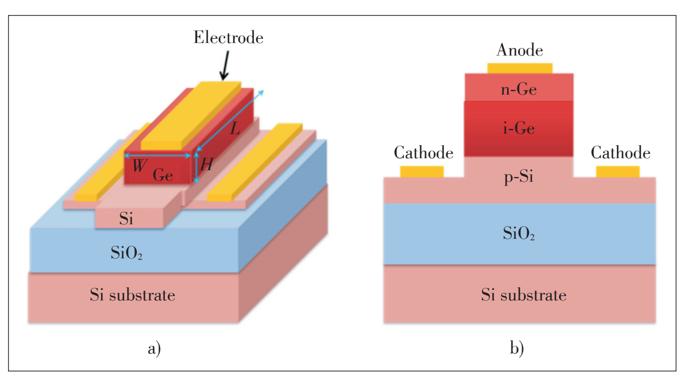

▲**Figure 7. a) The schematic structure and b) the cross-sectional image of the designed Ge photodetector.**

electrode are the width of the signal line (W) and the gap between signal line and ground line (G) as shown in Fig. 1.

Since the devices are designed for the 100 Gb/s coherent system, the bandwidth of the modulator is required to be larger than 23 GHz. Considering the insertion loss, the length of the device are chosen to be 700 um. Optimizing the model by parameter sweeping, the change of the S_{21} parameter with W and G are described in **Fig. 4**. When W increases, the microwave loss decreases, which can broaden the bandwidth. Meanwhile, the characteristic impedance decreases with the increasing W, and the bandwidth decreases with the impedances' mismatch. When G increases, the interaction between signal and ground line decreases and results in less modulation and lower bandwidth.

When W is 70 μm and G is 5.3 μm, the travelling wave electrode has a lowest loss at 23 GHz. Then, the S parameter of this device was simulated. The S_{21} and S_{11} curves are shown in **Fig. 5**. The 3 dB electro-optical bandwidth of the modulator is nearly the 6 dB electric bandwidth of the travelling-wave electrode. Fig. 5 shows the 6 dB bandwidth of the electrode is roughly 30 GHz.

4 Design of PIN Waveguide Photodetector

For single mode propagation, we choose the height and the width of the rib waveguide 220 nm and 600 nm respectively, and the slab thickness is 60 nm. This waveguide can confine the single transverse electric (TE) mode well as **Fig. 6** shows.

The schematic structure and the cross-sectional image of the designed Ge photodetector are shown in **Fig. 7**.

Here we assume the refractive index of the Ge is 4.275 + 0.02835j at C-band. Simulation results show that when the length of the Ge (L) reached a certain level, the light absorption would not increase with the length. Therefore we optimized the length of the Ge layer as shown in **Fig. 8**.

When the length reaches 10 um, the light absorption becomes saturated. Since the larger the device area, the smaller the bandwidth limitation, we chose 10 μm as the device length (L). Moreover, the width of the Ge layer (W) is designed to be 1.6 μm so that high bandwidth can be obtained simultaneously. According to the fabrication situation of the foundry, we follow the same thickness of the Ge layer (H) as 500 nm.

The cathode and anode contacts can be defined in the contacts table and set to simulate a single bias of -1 V in DEVICE module, after importing the photon-generated carriers file gen-

D:\EMAG\2017-08-58/VOL15\RP3.VFT——6PPS/P4

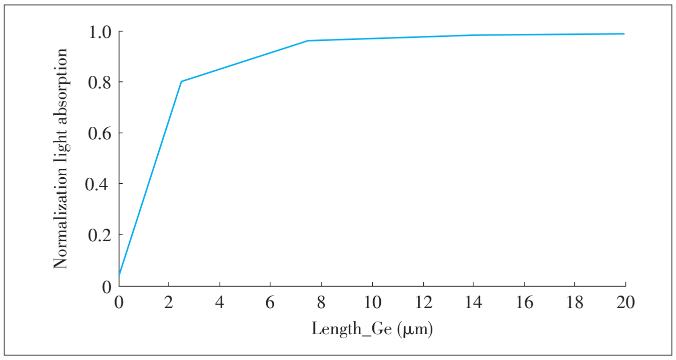

▲**Figure 8. Normalization light absorption vs. the length of Ge characteristic.**

erated by the FDTD simulation. The PIN photo detector is defined by n^{++} type, p^{+} type and p^{++} type implants in the Ge with peak doping density of 1×10^{20} /cm^3, 3×10^{18} /cm^3 and 1×10^{20} /cm^3. **Figs. 9–11** show the dark current of 16 nA at -1 V, responsivity of 1 A/W at -1 V over the C band, and 3 dB bandwidth of 26 GHz at -3 V respectively. The Ge photodetector we have designed can be readily used in the high speed optical

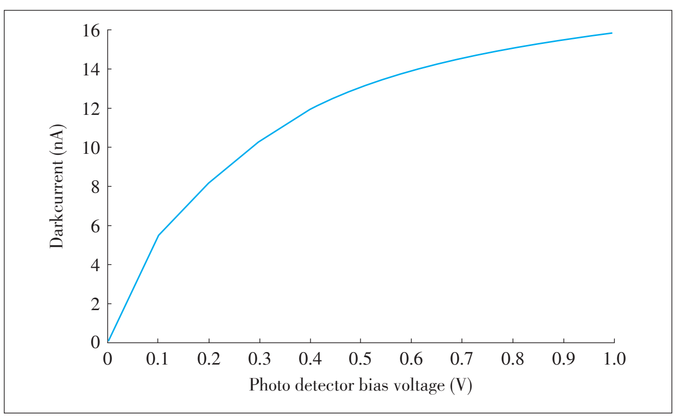

▲**Figure 9. Dark current of the designed Ge photo detector at different reverse biases.**

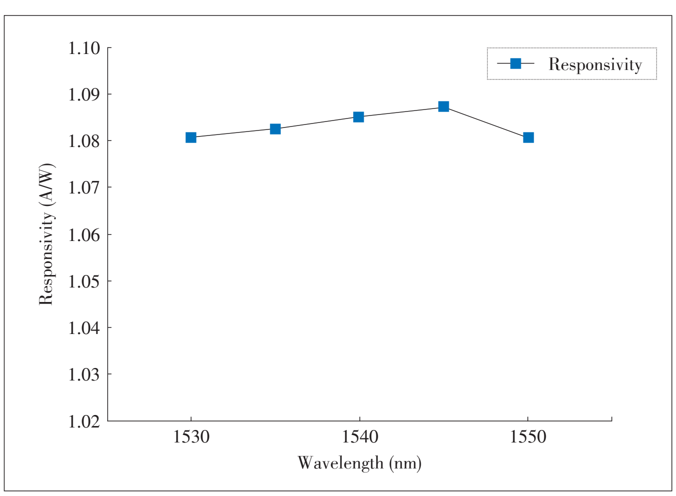

▲**Figure 10. Spectral responsivity of the designed Ge photo detector.**

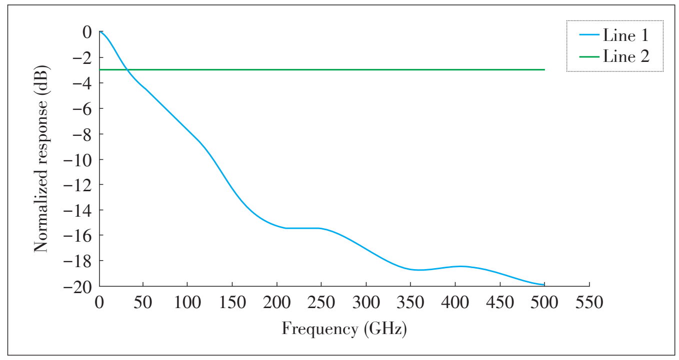

▲**Figure 11. 3 dB bandwidth of the designed Ge photo detector (Line 1) -3 V (Line 2).**

transmission systems of 100 Gb/s and beyond.

5 Conclusions

The silicon Mach-Zehnder modulator and PIN waveguide photodetector were analyzed and designed. The modulator with 700 μm long optimized U-type PN junction has high modulation efficiency and bandwidth. The extinction ratio of larger than 20 dB and the insertion loss of less than 5 dB are also acceptable. The PIN waveguide photo detector has high performance and the dark current is only about 16 nA at -1 V, responsivity is more than 1 A/W at -1 V over the C band, and 3 dB bandwidth is more than 26 GHz at -3 V. The performance of the silicon Mach-Zehnder modulator and Ge PIN waveguide photo detector designed can be sufficiently suitable in the commercial 100 Gb/s optical transmission system. The silicon devices bring the highly integrated and low-cost 100 Gb/s optical systems.

Acknowledgements

All the authors would like to acknowledge LI Tiantian (Peking University), TU Zhijuan (Peking University), and ZHANG Qi (ZTE Corporation) for their participation and support to this collaborative project.

References

[1] D. A. B. Miller, "Device requirements for optical interconnects to silicon chips," *Proc. IEEE*, vol. 97, no. 7, pp. 1166–1185, Jul. 2009. doi: 10.1109/JPROC.2009.2014298.

[2] D. Ahn, C. Hong, J. Liu, et al., "High performance, waveguide integrated Ge photo detectors," *Optics Express*, vol. 15, no 7, pp. 3916–3921, 2007. doi: 10.1364/OE.15.003916.

[3] Q. Xu, B. Schmidt, S. Pradhan, and M. Lipson, "Micrometre-scale silicon electro-optic modulator," *Nature*, vol. 435, no. 7040, pp. 325–327, 2005. doi: 10.1038/nature03569.

[4] B. Jalali and S. Fathpour, "Silicon photonics," *Journal of Lightwave Technology*, vol. 24, no. 12, pp. 4600–4615, 2006. doi: 10.1109/JLT.2006.885782.

[5] G. T. Reed, G. Mashanovich, F. Y. Gardes, and D. J. Thomson, "Silicon optical modulators," *Nature Photonics*, vol. 4, no. 8, pp. 518–526, Jul. 2010. doi: 10.1038/nphoton.2010.179.

[6] A. E. J. Lim, J. Song, F. Qing, C. Li, et al., "Review of silicon photonics foundry efforts," *IEEE Journal of Selected Topics in Quantum Electronics*, vol. 20, no. 4, pp. 405–416, 2014. doi: 10.1109/JSTQE.2013.2293274.

[7] A. R. Chralyvy, "The coming capacity crunch," in *35th European Conference on Optical Communication*, Vienna, Austria, 2009.
[8] R. W. Tkach, "Scaling optical communications for the next decade and beyond," *Bell Labs Technical Journal*, vol. 14, pp. 3–10, 2010. doi: 10.1002/bltj.20400.
[9] A. D. Ellis, F. C. G. Gunning, B. Cuenot, T. C. Healy, and E. Pincemin, "Towards 1TbE using coherent WDM," in *Joint Conference of the Opto-Electronics and Communications Conference and the Australian Conference on Optical Fibre Technology*, Sydney, Australia, 2008. doi: 10.1109/OECCACOFT.2008.4610550.
[10] P. J. Winzer and R. Essiambre, "Advanced optical modulation formats," *Proceedings of the IEEE*, vol. 94, no. 5, pp. 952–985, May 2006. doi: 10.1109/JPROC.2006.873438.
[11] K. Kikuchi, "Digital coherent optical communication systems: fundamentals and future prospect," *IEICE Electron. Express*, vol. 8, no. 20, pp. 1642–1662, 2011. doi: 10.1587/elex.8.1642.
[12] H. Yi, Q. Long, W. Tan, et al., "Demonstration of low power penalty of silicon Mach-Zehnder modulator in long-haul transmission," *Optics. Express*, vol. 20, no. 25, pp. 27562–27568, 2012. doi: 10.1364/OE.20.027562.
[13] T. Li, J. Zhang, H. Yi, et al., "Low-voltage, high speed, compact silicon modulator for BPSK modulation," *Optics. Express*, vol. 21, no. 20, pp. 23410–23415, 2013. doi: 10.1364/OE.21.023410.
[14] T. Li, J. Zhang, H. Yi, et al., "10-Gb/s 53.1-km BPSK transmission of silicon Mach-Zehnder modulator," in *Asia Communications and Photonics Conference*, Beijing, China, 2013. doi: 10.1364/ACPC.2013.AW4A.3.
[15] T. Li, D. Wang, J. Zhang, et al., "Demonstration of 6.25 Gbaud advanced modulation formats with subcarrier multiplexed technique on silicon Mach-Zehnder modulator," *Optics Express*, vol. 22, no. 16, pp. 19818–19823, 2014. doi: 10.1364/OE.22.019818.
[16] M. Cignoli, G. Minoia, M. Repossi, et al., "22.9 A 1310 nm 3D-integrated silicon photonics Mach-Zehnder-based transmitter with 275 mW multistage CMOS driver achieving 6 dB extinction ratio at 25 Gb/s," in *IEEE International Solid-State Circuits Conference*, San Francisco, USA, 2015. doi: 10.1109/ISSCC.2015.7063103.
[17] M. Nedeljkovic, R. A. Soref, and G. Z. Mashanovich, "Free-carrier electro-absorption and electro-refraction modulation in group IV materials at mid-infrared wavelengths," in *Proc. SPIE 8266 of Silicon Photonics VII*, San Francisco, USA, 2012. doi:10.1117/12.908650.
[18] J. F. Liu, D. Pan, S. Jongthammanurak, et al., "Design of monolithically integrated GeSi electro-absorption modulators and photo detectors on a SOI platform," *Optics Express*, vol. 15, no. 2, pp. 623–628, 2007. doi: 10.1364/OE.15.000623.
[19] G. T. Reed and A. P. Knights, *Silicon Photonics: An Introduction*. Chichester, England: John Wiley & Sons, 2004. doi: 10.1002/0470014180.
[20] C. T. DeRose, D. C. Trotter, W. A. Zortman, et al., "Ultra compact 45 GHz CMOS compatible Germanium waveguide photodiode with low dark current," *Optics Express*, vol. 19, no. 25, pp. 24897–24904, 2011. doi: 10.1364/OE.19.024897.
[21] L. Vivien, A. Polzer, D. M. Morini, et al., "Zero-bias 40 Gbit/s germanium waveguide photo detector on silicon," *Optics Express*, vol. 20, no. 2, pp. 1096–1101, 2012. doi:10.1364/OE.20.001096.
[22] L. P. Virot, L. Vivien, J. M. Fedeli, et al., "High-performance waveguide-integrated germanium PIN photodiodes for optical communication applications," *Photon. Research*, vol. 1, no. 3, pp. 140–147, 2013. doi: 10.1364/PRJ.1.000140.
[23] Z. Tu, K. Liu, H. Yi, et al., "A Compact Evanescently-coupled Germanium PIN Waveguide Photo detector," in *Proc. SPIE* 8564 *of Nanophotonics and Micro/Nano Optics*, Beijing, China, 2012. doi:10.1117/12.2001221.

Manuscript received: 2016-12-12

Biographies

ZHONG Fang (fzhong@pku.edu.cn) received the B.E. degree in materials engineering from Peking University, China in 2015. Since 2015, he has been working for his master degree at the State Key Laboratory of Advanced Optical Communication Systems and Networks, School of Electronics Engineering and Computer Science, Peking University, China. His current research interests include silicon based modulators and monolithic integration of high speed transmitters for optical communication systems.

GONG Pan (pankung@pku.edu.cn) received the B.E. degree in electronic from Hebei University of Engineering, China in 2012. He has obtained his master degree from the School of Software and Microelectronics, Peking University, China. His research interests include silicon-based Germanium photodetectors and monolithic integration of high speed coherent receivers for optical communication systems.

ZHOU Zhiping (zjzhou@pku.edu.cn) received the Ph.D. degree in electrical engineering from Georgia Institute of Technology (GT), USA in 1993. From 1993 to 2005, he was with the Microelectronics Research Center at GT, where he engaged research and development in the areas of nanotechnology, integrated optoelectronics, nanophotonic devices, and semiconductor devices. He is currently a Changjiang Professor at Peking University, China, focusing on silicon photonics and microsystems research. He has been credited for more than 360 technical papers and presentations, and 15 patents. He was the Chair of IEEE Wuhan Section, 2007–2008, the Director of IEEE Atlanta Section, 2001–2003. He also chaired, cochaired, and served on many program committees for various conferences for OSA, IEEE Photonics Society, and SPIE. Dr. Zhou is a Fellow of OSA, SPIE, and IET, and a Life Member of PSC. He serves as the Editor-in-Chief of *Photonics Research* and is on OSA Board of Editors.

HUA Feng (hua.feng@zte.com.cn) received her master degree in optical instrument from Tianjin University, China in 1996. She has worked with ZTE Corporation since 2000. Currently she is a senior engineer focusing on advanced research of cutting-edge optical communication technologies include silicon photonics, SDM, and optical backplane. She has more than 10 patents.

WANG Huitao (wang.huitao@zte.com.cn) received the B.E. degree in electronic science and technology from Harbin Engineering University, China in 2000 and the M.S. degree in physical electronics from Beijing Insititute of Technology, China in 2003. He worked at ZTE Corporation from 2003 to 2017 and was responsible for the technical planning of optical network system and optoelectronics devices. He has been working with ZTE Photonics since 2017, and is committed to the research and planning of high-speed optoelectronic devices in optical communications.

D:\EMAG\2017-08-58/VOL15\RP3.VFT——6PPS/P6